

# D ynam ics of netw orks and applications

R . V ilela M endes  
 G rupo de F ísica-M atem ática  
 C om plexo Interdisciplinar, U niversidade de Lisboa  
 A v. G am a P into, 2, 1699 Lisboa C odex Portugal  
 e-m ail: vilela@alf4.ci.fc.ul.pt

## A bstract

A survey is made of several aspects of the dynam ics of networks, with special em phasis on unsupervised learning processes, non-G aussian data analysis and pattern recognition in networks with com plex nodes.

## C ontents

1	R ecurrent networks. D ynam ics and applications	1
2	U nsupervised learning in generalized networks and the process- ing of non-G aussian signals	4
2.1	U nsupervised learning in general networks . . . . .	4
2.1.1	H ebbian -type learning with a node param eter . . . . .	5
2.2	N on-G aussian data and the neural com putation of the character- istic function . . . . .	10
3	C haotic networks for inform ation processing	18
3.1	A network of Bemoulli units . . . . .	20
3.2	Feigenbaum networks . . . . .	24
3.2.1	A simple system with an in nite number of sinks . . . . .	26
3.2.2	Feigenbaum networks with m any units . . . . .	26

## 1 R ecurrent networks. D ynam ics and applica- tions

There are three large classes of neural networks. One is the class of m ultilayered feedforward networks which, through supervised learning, are used to approxi-  
mate nonlinear functions. The second is the class of relaxation networks with sym-  
metric synaptic connections, like the Hop eld network. Under time evolu-  
tion the relaxation networks evolve to xed points which, in successful applica-  
tions, are identi ed with m em orized patterns. In the last class one includes all

networks with arbitrary connections which are neither completely feedforward nor symmetric. They are called recurrent networks.

Recurrent networks exhibit a complex variety of temporal behavior and are increasingly being proposed for use in many engineering applications [1] [2] [3] [4]. In contrast to feedforward or relaxation networks, the rich dynamical structure of recurrent networks makes them a natural choice to process temporal information. Even for the learning of nonlinear functions the feedback structure improves the reproduction of discontinuities or large derivative regions [5]. Also, in some cases, the feedback structure is a way to enhance, through a choice of architecture, the sensitivity of the network to particular features to be detected [6]. The learning algorithms used for feedforward networks may be generalized to the recurrent case [7] [8] [9] [6]. Some of this will be covered by another speaker at this conference.

Feedback loops and coexistence of quiescent, oscillatory and chaotic behavior are also present in biological systems and only the recurrent networks are appropriate models for these phenomena [10] [11].

The whole field of recurrent networks, both for engineering and biological applications, is developing in many directions. Their global analysis is rather involved [12]. Their characterization as dynamical systems is sharpened by a decomposition theorem. Continuous state - continuous time neural networks, as well as many other systems [13], may be written in the Cohen-Grossberg [14] form

$$\frac{dx_i}{dt} = a_i(x_i) \left[ b_i(x_i) - \sum_{j=1}^n w_{ij} d_j(x_j) \right]; \quad (1)$$

Dynamical systems of this type have a decomposition property. Define

$$\begin{aligned} w_{ij} &= w_{ij}^{(S)} + w_{ij}^{(A)} \\ w_{ij}^{(S)} &= \frac{1}{2} (w_{ij} + w_{ji}) \\ w_{ij}^{(A)} &= \frac{1}{2} (w_{ij} - w_{ji}) \\ V^{(S)} &= \sum_{i=1}^n R_{x^i} b_i(x_i) d_i(x_i) + \frac{1}{2} \sum_{j,k=1}^n w_{jk}^{(S)} d_j(x^j) d_k(x^k) \\ H &= \sum_{i=1}^n R_{x^i} \frac{d_i(x_i)}{a_i(x_i)} d_i(x_i) \end{aligned} \quad (2)$$

Then we have the following

**Theorem [15]** If  $a_i(x_i) = d_i(x_i) > 0 \forall x_i$  and the matrix  $w_{ij}^{(A)}$  has an inverse then the vector field  $\dot{x}_i$  in Eq.(1) decomposes into one gradient and one Hamiltonian components,  $\dot{x}_i = \dot{x}_i^{(G)} + \dot{x}_i^{(H)}$ , where

$$\begin{aligned} \dot{x}_i^{(G)} &= \frac{a_i(x_i)}{d_i(x_i)} \frac{\partial V^{(S)}}{\partial x_i} = \sum_j^P g^{ij}(x) \frac{\partial V^{(S)}}{\partial x_j} \\ \dot{x}_i^{(H)} &= \sum_j^P a_i(x_i) w_{ij}^{(A)}(x) a_j(x_j) \frac{\partial H}{\partial x_j} = \sum_j^P I^{ij}(x) \frac{\partial H}{\partial x_j} \end{aligned} \quad (3)$$

and

$$\begin{aligned} g^{ij}(\mathbf{x}) &= \frac{a_i(\mathbf{x}_i)}{d_i^0(\mathbf{x}_i)} \delta_{ij} \\ \omega_{ij}(\mathbf{x}) &= a_i(\mathbf{x}_i)^{-1} w^{(A)}_{ij}(\mathbf{x}) a_j(\mathbf{x}_j)^{-1} \end{aligned} \quad (4)$$

$\omega_{ij} I^{jk} = \delta_{ij}^k \cdot g^{ij}(\mathbf{x})$  and  $\omega_{ij}(\mathbf{x})$  are the components of the Riemannian metric and the symplectic form.

Proof: The decomposition follows by direct calculation from (1) and (2). The conditions on  $a_i(\mathbf{x}_i)$ ,  $d_i^0(\mathbf{x}_i)$  and  $w^{(A)}$  insure that  $g$  is a well defined metric and  $\omega$  is non-degenerate. Indeed let  $v$  be a vector such that  $\omega_{ij} v^i = 0$ . Then

$$0 = \sum_{ij} v^i \omega_{ij} a_j(\mathbf{x}_j) w_{jk}^{(A)}(\mathbf{x}) = \frac{v^k}{a_k(\mathbf{x}_k)}$$

would imply  $v^k = 0 \quad \forall k$ . That  $\omega$  is a closed form follows from the fact that  $\omega_{ij}$  depends only on  $\mathbf{x}_i$  and  $\mathbf{x}_j$ .

The identification, in the system (1), of just one gradient and one Hamiltonian component with explicitly known potential and Hamiltonian functions, is a considerable simplification as compared to a generic dynamical system. Recall that in the general case, although such a decomposition is possible locally [16], explicit functions are not easy to obtain unless one allows for one gradient and  $n-1$  Hamiltonian components. Notice that the decomposition of the vector field does not decouple the dynamical evolution of the components. In fact it is the interplay of the dissipative (gradient) and the Hamiltonian component that leads, for example, to limit cycle behavior.

For the case of symmetric connections  $w_{ij} = w_{ji}$  one recovers the Cohen-Grossberg result [14] that states that a symmetric system of the type of Eq.(1) has a Lyapunov function  $V^{(S)}$  of which Hopfeld's [17] "energy" function is a particular case. For the symmetric case the existence of a Lyapunov function guarantees global asymptotic stability of the dynamics. However not all vector fields with a Lyapunov function are differentially equivalent to a gradient field. Therefore the fact that a gradient vector is actually obtained gives additional information, namely about structural stability of the model.

A necessary condition for structural stability of the gradient vector field is the non-degeneracy of the critical points of  $V^{(S)}$ , namely  $\det \frac{\partial^2 V^{(S)}}{\partial x_i \partial x_j} \neq 0$  at the points where  $\frac{\partial V^{(S)}}{\partial x_i} = 0$ . In a gradient flow all orbits approach the critical points as  $t \rightarrow \infty$ . If the critical points are non-degenerate then the gradient flow satisfies the conditions defining a Morse-Smale field, except perhaps the transversality conditions for stable and unstable manifolds of the critical points. However because Morse-Smale fields are open and dense in the set of gradient vector fields, any gradient flow with non-degenerate critical points may always be  $C^1$ -approximated by a (structurally stable) Morse-Smale gradient field. Therefore given a symmetric model of the type (1), the identification of its gradient nature provides a easy way to check its robustness as a physical model.

As an example of the decomposition applied to a biological model consider the Wilson-Cowan model of a neural oscillator without refractory periods, in the antisymmetric coupling case considered by most authors

$$\begin{aligned} \dot{x}_1 &= -x_1 + S(x_1 + w_{11}x_1 + w_{12}x_2) \\ \dot{x}_2 &= -x_2 + S(x_2 + w_{21}x_1 + w_{22}x_2) \end{aligned} \quad (5)$$

with  $w_{12} = -w_{21}$  and  $S$  is the sigmoid function  $(1 + e^{-x})^{-1}$ . Changing variables to

$$z_i = x_i + \sum_{j=1}^2 w_{ij}x_j$$

one obtains

$$\begin{aligned} \dot{z}_1 &= \frac{\partial V}{\partial z_1} + w_{12} \frac{\partial H}{\partial z_2} \\ \dot{z}_2 &= \frac{\partial V}{\partial z_2} - w_{12} \frac{\partial H}{\partial z_1} \end{aligned} \quad (6)$$

with

$$\begin{aligned} V &= \frac{1}{2} \sum_i z_i^2 - \sum_i z_i + w_{ii} \log(1 + S(z_i)) \\ H &= \sum_i \log(1 + S(z_i)) \end{aligned}$$

The model is completely described by these functions, the bifurcation sets [18], for example, being characterized by  $\det D^2V = 0$  for Andronov-Hopf bifurcations and by

$$\frac{\partial^2 V}{\partial z_1^2} \frac{\partial^2 V}{\partial z_2^2} + w_{12}^2 \frac{\partial^2 H}{\partial z_1^2} \frac{\partial^2 H}{\partial z_2^2} = 0$$

for saddle-node bifurcations.

## 2 Unsupervised learning in generalized networks and the processing of non-Gaussian signals

### 2.1 Unsupervised learning in general networks

Doyle Farmer [19] has shown that there is a common mathematical framework where neural networks, classical systems, immune networks and autocatalytic reaction networks may be treated in a unified way. The general model in which all these models may be mapped looks like a neural network where, in addition to the node state variables ( $x_i$ ) and the connection strengths ( $w_{ij}$ ), there is also a node parameter ( $\theta_i$ ) with learning capabilities (Fig. 1). The node parameter represents the possibility of changing, through learning, the nature of the linear or non-linear function  $f_i(\sum_j w_{ij}x_j)$  at each node. In the simplest case  $\theta_i$  will be simply an intensity parameter. Therefore the degree to which the activity at node  $i$  influences the activity at other nodes depends not only on the connection strengths ( $w_{ij}$ ) but also on an adaptive node parameter  $\theta_i$ . In some cases, as in the B-cell immune network, the node parameter is the only means to control the relative influence of a node on others, the connection strengths being fixed chemical reaction rates.

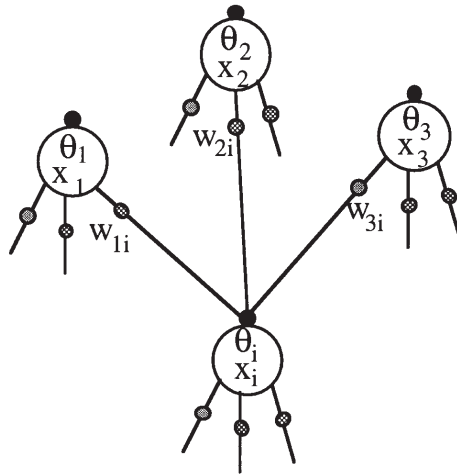


Figure 1: A general connectionist network with state variables ( $x_i$ ), connection strengths ( $w_{ij}$ ) and node parameters ( $\theta_i$ )

### 2.1.1 Hebbian - type learning with a node parameter

We will denote by  $x_i$  the output of node  $i$ . Hebbian learning [20] is a type of unsupervised learning where a connection strength  $w_{ij}$  is reinforced whenever the product  $x_i x_j$  is large. As shown by several authors, Hebbian learning extracts the eigenvectors of the correlation matrix  $Q$  of the input data.

$$Q_{ij} = \langle x_i x_j \rangle \quad (7)$$

where  $\langle \cdot \rangle$  means the sample average. If the learning law is local, the lines of the connection matrix  $w_{ij}$  all tend to the eigenvector associated to the largest eigenvalue of the correlation matrix. To obtain the other eigenvector directions one needs non-local laws [21] [22] [23]. Sanger's approach has the advantage of organizing the connection matrix in such a way that the rows are the eigenvectors associated to the eigenvalues in decreasing order. It suffers however from slow convergence rates for the lowest eigenvalues. The methods that have been proposed may, with some modifications, be used both for linear and non-linear networks. However, because the maximum information about a signal  $f(x)$ , that may be coded directly in the connection matrix  $w_{ij}$ , is the principal components decomposition and this may already be obtained with linear units, we will discuss only this case.

The learning rules proposed below [24] are a generalization of Sanger's scheme including a node parameter  $\theta_i$ . We consider a one-layer feedforward network with as many inputs as outputs (Fig 2) and the updating rules proposed for

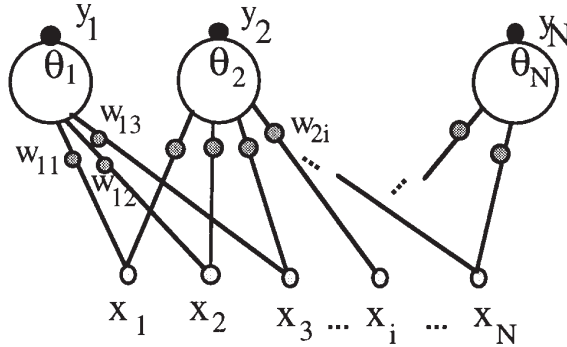


Figure 2: One-layer neural feedforward network for Hebbian learning with node parameter

$W_{ij}$  and  $\theta_i$  are:

$$\begin{aligned} W_{ij}(t+1) &= W_{ij}(t) + \eta y_i(t) x_j(t) \\ \theta_i(t+1) &= \theta_i(t) + \eta y_i(t) f(\theta_i(t)) \end{aligned} \quad (8)$$

where  $y_i$  is the output of node  $i$

$$y_i = \sum_j W_{ij} x_j \quad (9)$$

and  $\eta$  and  $\alpha$  are positive constants that control the learning rate. As will be shown below the learning dynamics of Eqs(8) has the capability to accelerate the convergence rate for the small eigenvalues of  $Q$ . To avoid undesirable fixed points of the dynamics, where this acceleration effect is not obtained, the learning rules (8) are supplemented by the following prescription: The starting  $\theta_i$ 's are all positive and are not allowed to decrease below a value  $(\theta_i)_{min}$ . If, at a certain point of the learning process,  $\theta_i$  hits the lower bound then one makes the replacement  $W_{ij} \rightarrow W_{ij} - \alpha W_{ij}$  in the line  $i$  of the connection matrix (see remark 3).

Define the  $N$ -dimensional vectors

$$\begin{aligned} (x)_i &= x_i \\ (W_i)_j &= W_{ij} \end{aligned} \quad (10)$$

Then the following result was proven [24]:

If the time scale of the system (8) is much slower than the averaging time of the input signal  $x_i(t)$  then:

a) the system (8) has a stable fixed point such that

$$\begin{aligned} Q W_i &= -\theta_i W_i \\ \theta_i &= \frac{1}{\alpha} \langle W_i \cdot x \rangle \end{aligned} \quad (11)$$

and  $\sum_{i,j} W_{ij} = 1$ .  $\lambda_i > 0$  ( $i=1, \dots, N$ ) are the eigenvalues of the correlation matrix.

b) Convergence to the fixed point is sequential in the sense that  $W_i$  is only attracted to the eigenvector described in (11) if all vectors  $W_j$  for  $j < i$  are already close to their corresponding eigenvector values.

Remarks:

1 - The matrix  $W$  of the connection strengths extracts the principal components of the correlation matrix  $Q$ . The node parameters  $W_i$  at their fixed point (11) extract additional information on the mean value of the data vector  $x$  and the eigenvalues of  $Q$ . To deal with data with zero mean it is convenient to change the  $W_i$  updating law to

$$W_i(t+1) = W_i(t) + \frac{1}{N} \sum_k W_{ij}(x_k + r_k) - W_{ik} x_k; \quad (12)$$

where  $r$  is a fixed vector.

The stable fixed point is now

$$W_i = \frac{1}{N} (W_i (\langle x \rangle + r)) \quad (13)$$

If one wishes to separate the eigenvalues from the information on the average data  $\langle x \rangle$  one may add another parameter  $W_i$  to each node with a learning law

$$W_i(t+1) = W_i(t) + \frac{1}{N} \sum_k W_{ik} x_k; \quad (14)$$

which, with the same assumptions about time scales as before, converges to the stable fixed point

$$W_i = \frac{1}{N} \lambda_i \quad (15)$$

The convergence rate near the fixed point is  $\frac{1}{N}$ . Therefore choosing a large  $N$  accelerates convergence for the small eigenvalues.

2 - In addition to its role in extracting additional information on the input signal, the node parameters  $W_i$  also plays a role in accelerating the convergence to the stable fixed point. For fixed  $W_{ij}$ , the rate of convergence to the fixed point is very slow for the components associated to the smallest eigenvalues. This is the reason for the convergence problems in Sanger's method and one also finds that sometimes the results for the small components are quite misleading. On the other hand to increase  $W_{ij}$  does not help because then the time scale of the  $W_{ij}$  learning law becomes of the order of the time scale of the data and one obtains large fluctuations in the principal components. With a node parameter and the learning law (8) the situation is more favorable because for small eigenvalues the effective control parameter ( $W_i$ ) is dynamically amplified. This accelerates

the convergence of the minor components without inducing fluctuations on the principal components.

3- Here one examines the effect of the prescription to avoid the fixed points where some  $e_i = 0$ . Consider the average evolution of  $\theta_i$ , assuming all the other variables fixed

$$\theta_i(t+1) = \theta_i(t) (1 + W_i \langle x \rangle) - \theta_i^2(t) (W_i \circ W_i)$$

If  $W_i \langle x \rangle > 0$  the stable fixed point is at  $W_i \langle x \rangle = (W_i \circ W_i)$  and if  $W_i \langle x \rangle < 0$  it is at zero (see Fig.3). If  $W_i \langle x \rangle$  is  $< 0$ ,  $\theta_i$  moves towards

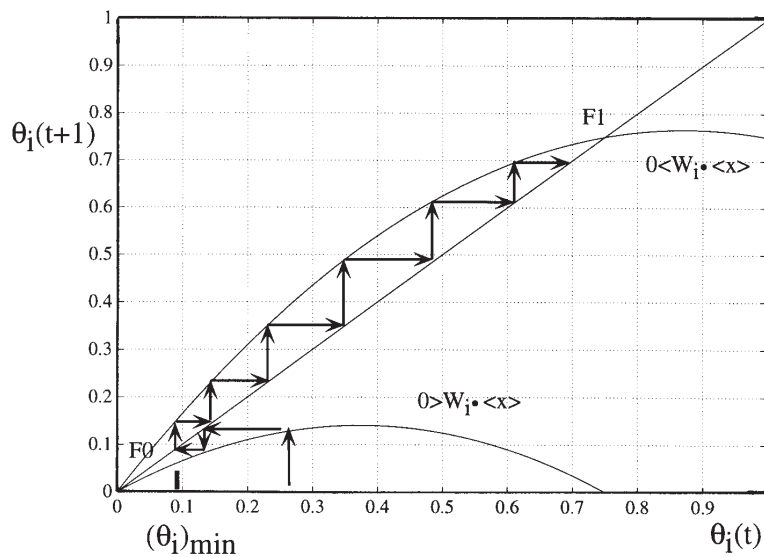


Figure 3: The effect of changing the sign of  $W_i$  in the approach to the stable fixed points

the fixed point  $F_0$  at zero but, when it reaches  $(\theta_i)_{min}$ , the change in the sign of the corresponding row  $W_i$  in connection matrix changes the dynamics and it is  $F_1$  that is now the attracting fixed point.

To illustrate the effect of node parameters in principal component analysis (PCA), consider the following two-dimensional signal, where  $t_i$  are Gaussian distributed variables with zero mean and unit variance:

$$x_1 = t_1; x_2 = t_1 + 0.08t_2$$

The principal components of the signal and the eigenvalues are given in the following table.

$i$	$W_{i1}$	$W_{i2}$
2.0032	0.7060	0.7082
0.0032	0.7082	0.7060

A one-layer network with node parameters as in Fig.2 is used to perform PCA. Fig.4 shows the data and the principal directions that are obtained using

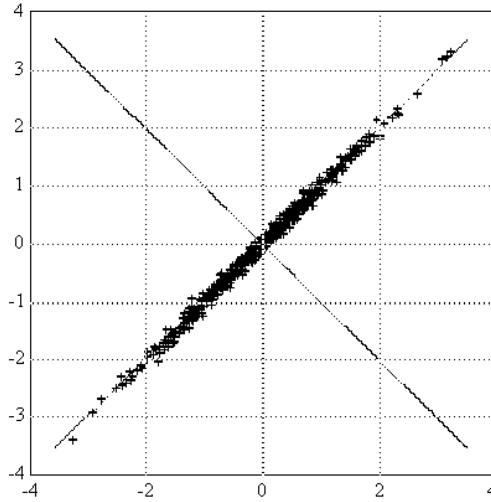


Figure 4: Signal distribution and its principal directions

the learning laws (8) and (12). The parameter values used are  $w = 0.015$ ,  $\alpha = 0.005$  and  $r = (0.002, 0.002)$ . Fig.5 shows the convergence of the  $W$ 's to their final values in the learning process. Fig.6 shows the variation of the node parameters.

Sanger's original algorithm is recovered by fixing the node parameters to unit values. In this case the principal components are also extracted, but the convergence of the process is much slower as shown in Fig.7. With node parameters, improved convergence of the small eigenvalues is to be expected under generic conditions because the rates of convergence are controlled by  $w_i$  and  $\alpha_i$  is proportional to  $\frac{1}{\lambda_i}$ . In the example the effect of  $\alpha_2$  is further amplified by the fact that, before  $W_2$  starts to converge,  $W_2$  error is large. Hence, in this case at least, the node parameter acts like a variable learning rate for the minor component. Notice that the method does not induce oscillations in the major components as would happen with large  $w$  values. Besides speeding up the learning process the node parameters also contain information about first moments and the eigenvalues.

Node parameters also have a beneficial effect on competitive learning algorithms. For details refer to [24].

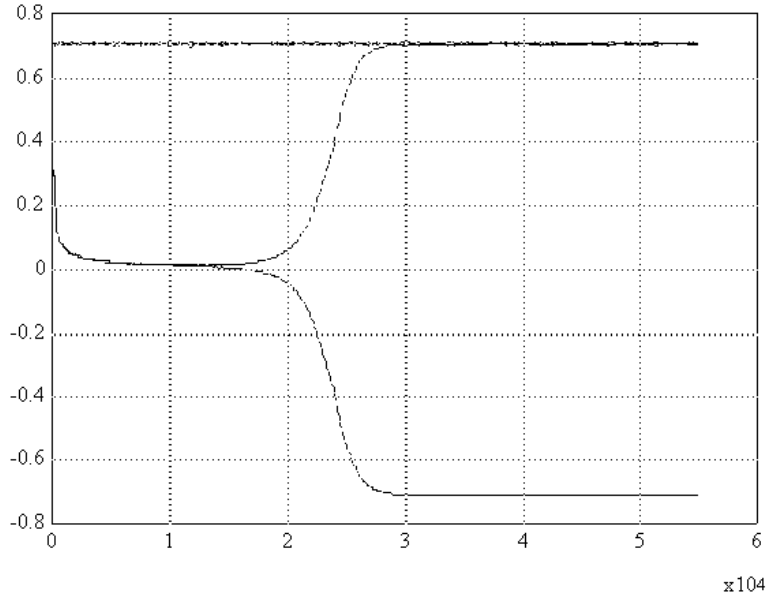


Figure 5: Evolution of  $W_1$  and  $W_2$

## 2.2 Non-Gaussian data and the neural computation of the characteristic function

The aim of principal component analysis (PCA) is to extract the eigenvectors of the correlation matrix, from the data. There are standard neural network algorithms for this purpose [21] [22] [23] [24]. However if the process is non-Gaussian, PCA algorithms or their higher-order generalizations provide only incomplete or misleading information on the statistical properties of the data.

Let  $x_i$  denote the output of node  $i$  in a neural network. Hebbian learning [20] is a type of unsupervised learning where the neural network connection strengths  $W_{ij}$  are reinforced whenever the products  $x_j x_i$  are large. The simplest form is

$$W_{ij} = x_i x_j \quad (16)$$

Hebbian learning extracts the eigenvectors of the correlation matrix  $Q$

$$Q_{ij} = \langle x_i x_j \rangle \quad (17)$$

but, if the learning law is local as in Eq.(16), all the lines of the connection matrix  $W_{ij}$  converge to the eigenvector with the largest eigenvalue of the correlation matrix. To obtain other eigenvector directions requires non-local laws. These principal component analysis (PCA) algorithms and the characteristic

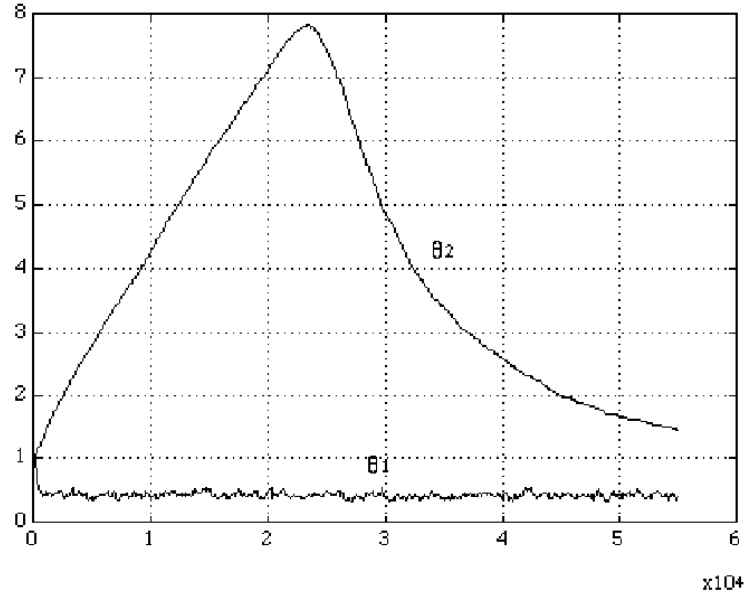


Figure 6: Evolution of  $\theta_1$  and  $\theta_2$

directions of the correlation matrix  $(Q)_{ij} = \langle x_i x_j \rangle$ . If the data has zero mean ( $\langle x_i \rangle = 0$ ) they are the orthogonal directions along which the data has maximum variance. If the data is Gaussian in each channel, it is distributed as a hyperellipsoid and the correlation matrix  $Q$  already contains all the information about statistical properties. This is because higher order moments of the data may be obtained from the second order moments. However, if the data is non-Gaussian, the PCA analysis is not complete and higher order correlations are needed to characterize the statistical properties. This led some authors [25] [26] to propose networks with higher order neurons to obtain the higher order statistical correlations of the data. A higher order neuron is one that is capable of accepting, in each of its input lines, data from two or more channels at once. There is then a set of adjustable strengths  $W_{i_1 i_2}; \dots; W_{i_1 \dots i_n}$ ,  $n$  being the order of the neuron. Networks with higher order neurons have interesting applications, for example in fitting data to a high-dimensional hypersurface. However there is a basic weakness in the characterization of the statistical properties of non-Gaussian data by higher order moments. Existence of the moments of a distribution function depends on the behavior of this function at infinity and it frequently happens that a distribution has moments up to a certain order, but no higher ones. A well-behaved probability distribution might even have no moments of order higher than one (the mean). In addition a sequence of moments does not necessarily determine a probability distribution function uniquely [27].

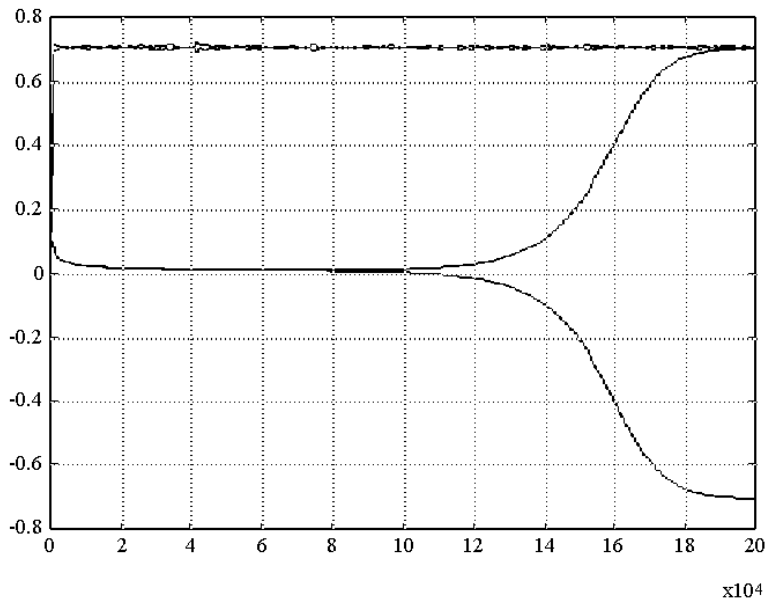


Figure 7: Evolution of  $W_1$  and  $W_2$  using Sanger's algorithm, without node parameters

Two different distributions may have the same set of moments. Therefore, for non-Gaussian data, the PCA algorithms or higher order generalizations may lead to misleading results.

As an example consider the two-dimensional signal shown in Fig.8. Fig.9 shows the evolution of the connection strengths  $W_{11}$  and  $W_{12}$  when this signal is passed through a typical PCA algorithm. Large oscillations appear and finally the algorithm overflows. Smaller learning rates do not introduce qualitative modifications in this evolution. The values may at times appear to stabilize, but large spikes do occur. The reason is that the seemingly harmless data in Fig.8 is generated by a linear combination of a Gaussian with the following distribution

$$p(x) = k(2 + x^2)^{-\frac{3}{2}} \quad (18)$$

which has first moment, but no moments of higher order.

To be concerned with non-Gaussian processes is not a pure academic exercise, because in many applications adequate tools are needed to analyze such processes. For example, processes without higher order moments, in particular those associated with Levy statistics, are prominent in complex processes such as relaxation in glassy materials, chaotic phase diffusion in Josephson junctions and turbulent diffusion [28] [29] [30]. Moments of an arbitrary probability distribution may not exist. However, because every bounded and measurable function

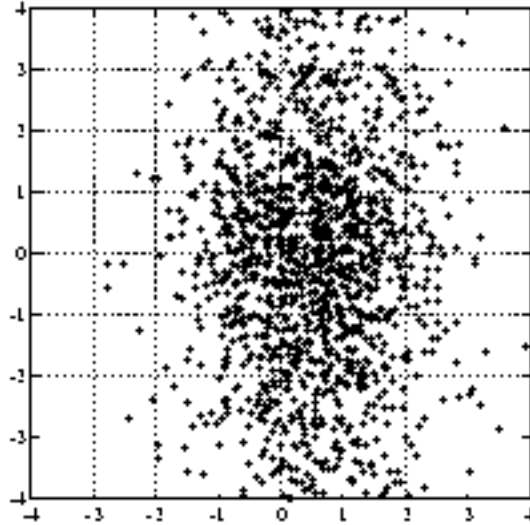


Figure 8: A two-dimensional test signal

is integrable with respect to any distribution, the existence of the characteristic function  $f(\cdot)$  is always assured [27].

$$f(\cdot) = \int_{\mathcal{Z}} e^{i \langle \cdot, x \rangle} dF(x) = \langle e^{i \langle \cdot, x \rangle} \rangle \quad (19)$$

and  $x$  are  $N$ -dimensional vectors,  $x$  is the data vector and  $F(x)$  its distribution function. The characteristic function is a compact and complete characterization of the probability distribution of the signal. If, in addition, one wishes to describe the time correlations of the stochastic process  $x(t)$ , the corresponding quantity is the characteristic functional [31]

$$F(\cdot) = \int_{\mathcal{Z}} e^{i \langle \cdot, x \rangle} d(x) \quad (20)$$

where  $\langle \cdot, x \rangle$  is a smooth function and the scalar product is

$$\langle \cdot, x \rangle = \int_{\mathcal{Z}} dt x(t) \cdot (\cdot) \quad (21)$$

$\langle \cdot, x \rangle$  being the probability measure over the sample paths of the process.

In the following I will describe an algorithm to compute the characteristic function from the data, by a learning process [32]. The main idea is that, in the end of the learning process, one has a neural network which is a representation

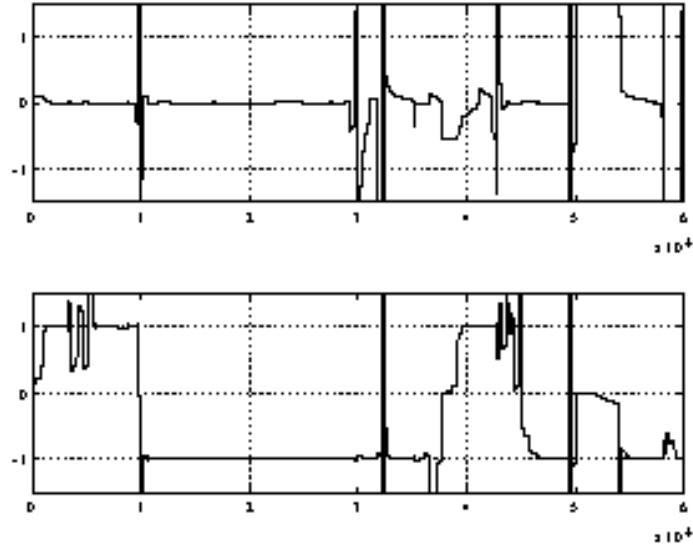


Figure 9: Evolution of the connection strengths  $W_{11}$  and  $W_{12}$  in a PCA network for the data in Fig.8

of the characteristic function. This network is then available to provide all the required information on the probability distribution of the data being analyzed.

Suppose we want to learn the characteristic function  $f(\cdot)$  of a one-dimensional signal  $x(t)$  in a domain  $\mathcal{X} \subset [0; N]$ . The domain is divided in  $N$  intervals by a sequence of values  $0; \tau_1; \tau_2; \dots; N$  and a network is constructed with  $N + 1$  intermediate layer nodes and an output node (Fig. 10).

The learning parameters in the network are the connection strengths  $W_{0i}$  and the node parameters  $\tau_i$ . The existence of the node parameter means that the output of a node in the intermediate layer is  $\tau_i(x)$ ,  $\tau_i$  being a non-linear function. The use of both connection strengths and node parameters in neural networks makes them equivalent to a wide range of other connectionist systems [19] and improves their performance in standard applications [24]. The learning laws for the network in Fig. 10 are:

$$W_{0i}(t+1) = W_{0i}(t) + \eta \left( \cos \tau_i x(t) - \tau_i(t) \right) \tau_i(t) \quad (22)$$

;  $\eta > 0$ . The intermediate layer nodes are equipped with a radial basis function

$$\tau_i(x) = \frac{e^{-\frac{(x - \tau_i)^2}{2\sigma_i^2}}}{\sum_{k=0}^N e^{-\frac{(x - \tau_k)^2}{2\sigma_k^2}}} \quad (23)$$

where in general one uses  $\sigma_i = \tau_i$  for all  $i$ . The output is a simple additive

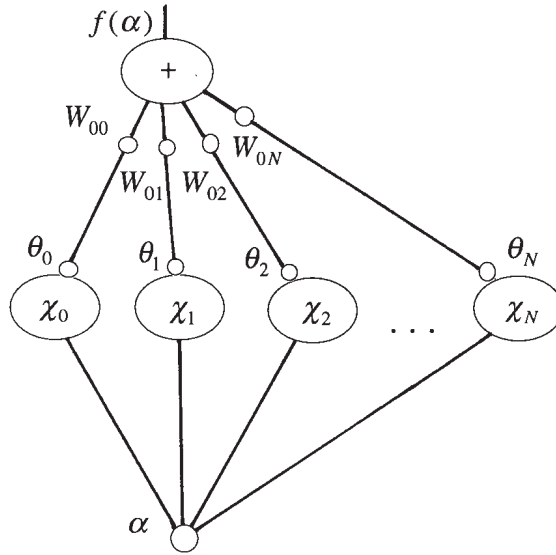


Figure 10: Network to learn the characteristic function of a scalar process

node. The learning constant should be sufficiently small to insure that the learning time is much smaller than the characteristic times of the data  $x(t)$ . If this condition is satisfied each node parameter  $\theta_i$  tends to  $\langle \cos \theta_i x \rangle$ , the real part of the characteristic function  $f(\cdot)$  for  $\theta = \theta_i$ . The  $W_{0i}$  learning law was chosen to minimize the error function

$$f(W) = \frac{1}{2} \sum_j \sum_k W_{0k}(t) \cos(\theta_j x_j(t)) \quad (24)$$

One sees that the learning scheme is an hybrid one, in the sense that the node parameter  $\theta_i$  learns, in an unsupervised way, (the real part of) the characteristic function  $f(\theta_i)$  and then, by a supervised learning scheme, the  $W_{0i}$ 's are adjusted to reproduce the  $\theta_i$  value in the output whenever the input is  $\theta_i$ . Through the learning law (22) each node parameter  $\theta_i$  converges to  $\langle \cos \theta_i x \rangle$  and the interpolating nature of the radialbasis functions guarantees that, after training, the network will approximate the real part of the characteristic function for any  $\theta$  in the domain  $[\theta_0; \theta_N]$ . A similar network is constructed for the imaginary part of the characteristic function, where now

$$\theta_i(t+1) = \theta_i(t) + (\sin \theta_i x(t) - \theta_i(t)) \quad (25)$$

For higher dimensional data the scheme is similar. The number of required nodes is  $N^d$  for a  $d$ -dimensional data vector  $x(t)$ . For example for the 2-dimensional data of Fig.8 a set of  $N^2$  nodes was used (Fig.11). Each node in the square

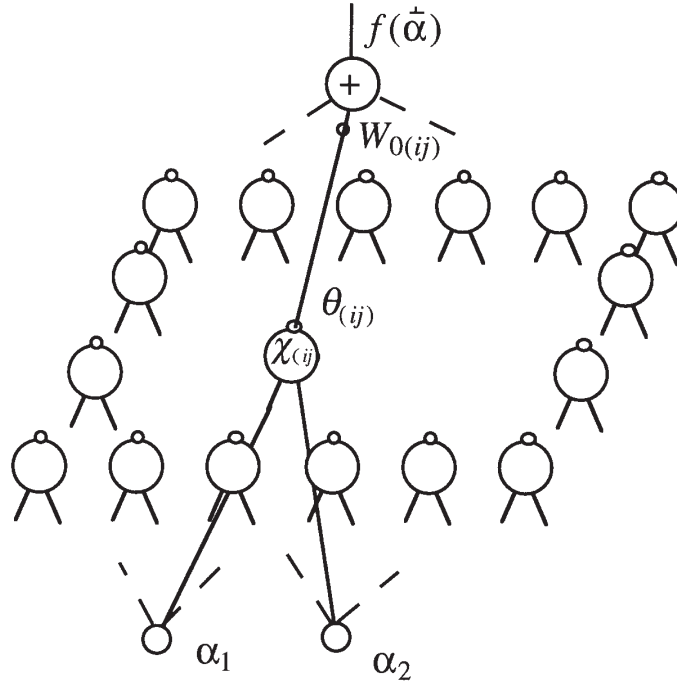


Figure 11: Network to learn the characteristic function of a 2-dimensional signal  $\mathbf{x}(t)$

lattice has two inputs for the two components  $\alpha_1$  and  $\alpha_2$  of the vector argument of  $f(\cdot)$ . The learning laws are, as before

$$\begin{aligned}
 \chi_{(ij)}(t+1) &= \chi_{(ij)}(t) + \cos \theta_{(ij)} \mathbf{x}(t) \cdot \chi_{(ij)}(t) \\
 W_{0(ij)}(t+1) &= W_{0(ij)}(t) + \\
 &+ \sum_{(k1)} \chi_{(k1)}(t) \sum_{(m n)} W_{0(m n)}(t) \chi_{(m n)}(\mathbf{x}(k1)) \chi_{(m n)}(t) \chi_{(ij)}(t) \chi_{(ij)}(\mathbf{x}(k1))
 \end{aligned}
 \tag{26}$$

The pair  $(ij)$  denotes the position of the node in the square lattice and the radial basis function is

$$\chi_{(ij)}(\mathbf{x}) = \frac{e^{-j \|\mathbf{x} - \mathbf{x}_{(ij)}\|^2}}{\sum_{(k1)} e^{-j \|\mathbf{x} - \mathbf{x}_{(k1)}\|^2}}
 \tag{27}$$

Two networks are used, one for the real part of the characteristic function, and another for the imaginary part with, in Eqs.(27),  $\cos \theta_{(ij)} \mathbf{x}(t) \cdot \chi_{(ij)}(t)$  replaced by  $\sin \theta_{(ij)} \mathbf{x}(t) \cdot \chi_{(ij)}(t)$ . Figs.12 and 13 show the values computed by the algorithm for the real and imaginary parts of the characteristic function corresponding to the two-dimensional signal in Fig.8.

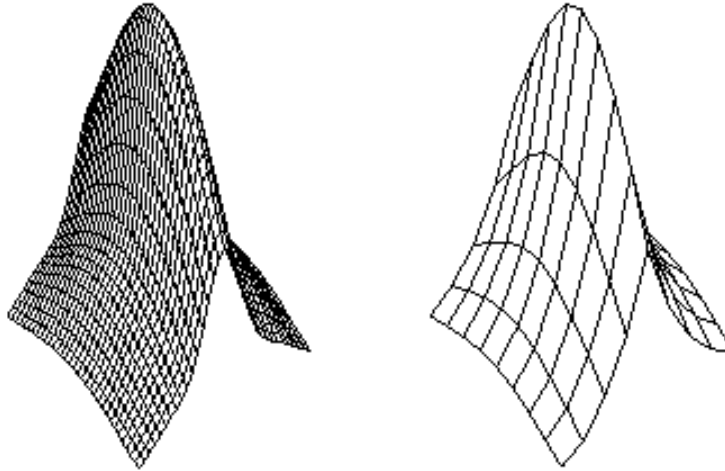


Figure 12: Real part of the characteristic function for the data in Fig. 8 (left) and the mesh of  $\xi_i$  values (right) obtained by the network

On the left is a plot of the exact characteristic function and on the right the values learned by the network. In this case we show only the mesh corresponding to the  $\xi_i$  values. One obtains a 2.0% accuracy for the real part and 4.5% accuracy for the imaginary part. The convergence of the learning process is fast and the approximation is reasonably good. Notice in particular the slope discontinuity at the origin which reveals the non-existence of a second moment.

For a second example the data was generated by a Weierstrass random walk with probability distribution

$$p(x) = \frac{1}{6} \sum_{j=0}^{\infty} \frac{2^{-j}}{3} x; b^j + x; b^j \quad (28)$$

and  $b=1.31$ , which is a process of the Levy flight type. The characteristic function, obtained by the network, is shown in Fig. 14.

Taking the  $\log(-\log)$  of the network output one obtains the scaling exponent 1.49 near  $\epsilon=0$ , close to the expected fractal dimension of the random walk path (1.5).

These examples test the algorithm as a process identifier, in the sense that, after the learning process, the network is a dynamical representation of the characteristic function and may be used to perform all kinds of analysis of the statistics of the data.

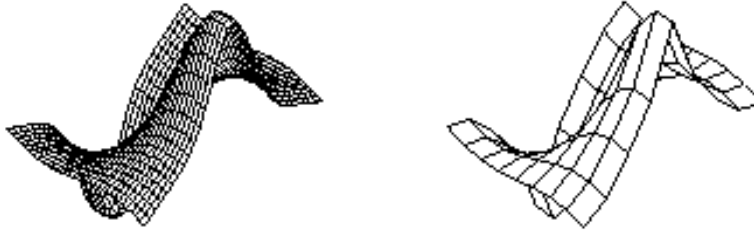


Figure 13: Imaginary part of the characteristic function for the data in Fig.8 (left) and the mesh of  $\phi$  values (right) obtained by the network

### 3 Chaotic networks for information processing

Freeman and collaborators [10] [33] [34] [35] [36] [37] have extensively studied and modeled the neural activity in the mammalian olfactory system. Their conclusions challenge the idea that pattern recognition in the brain is accomplished as in an attractor neural network [38]. Pattern recognition in the brain is the process by which external signals arriving at the sense organs are converted into internal meaningful states. The studies of the excitation patterns in the olfactory bulb of the rabbit lead to the conclusion that, at least in this biological pattern recognition system, there is no evolution towards an equilibrium fixed point nor does it seem to be minimizing an energy function. Other interesting conclusions of these biological studies are:

- the main component of the neural activity in the olfactory system is chaotic. This is also true in other parts of the brain, periodic behavior occurring only in abnormal situations like deep anesthesia, coma, epileptic seizures or in areas of the cortex that have been isolated from the rest of the brain;

- the low-level chaos that exists in absence of an external stimulus is, in the presence of a signal, replaced by bursts lasting for about 100 ms which have different intensities in different regions of the olfactory bulb. Olfactory pattern recognition manifests itself as a spatially coherent pattern of intensity;

- the recognition time is very fast, in the sense that the transition between different patterns occurs in times as short as 6 ms. Given the neuron characteristic response times this is clearly incompatible with the global approach to equilibrium of an attractor neural network;

- the biological measurements that have been performed do not record the action potential of individual neurons, but the local effect of the currents coming out of thousands of cells. Therefore the very existence of measurable activity bursts implies a synchronization of local assemblies of many neurons.

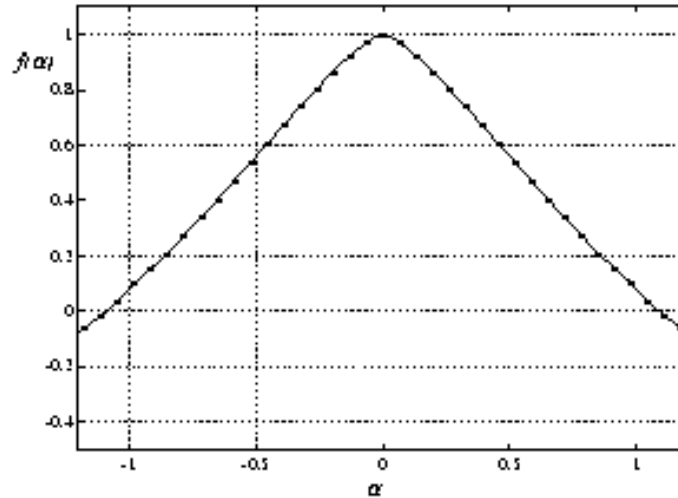


Figure 14: Characteristic function for the Weierstrass random walk ( $b=1.31$ )

Freeman, Yao and Burke[35] [36] model the olfactory system with a set of non-linear coupled differential equations, the coupling being adjusted by means of an input correlation learning scheme. Each variable in the coupled system is assumed to represent the dynamical state of a local assembly of  $m$  many neurons. Based on numerical simulations they conjecture that olfactory pattern recognition is realized through a multilobe strange attractor. The system would be, most of the time, in a basal (low-activity) state, being excited to one of the higher lobes by the external stimulus.

To compute or even prove the existence of chaotic measures in coupled differential equation systems is a awesome task. Therefore, even if it may be biologically accurate, the analytical model of these authors is difficult to deal with and unsuitable for wide application in technological pattern recognition tasks, although one such application has indeed been attempted by the authors[37]. However the idea that efficient pattern recognition may be achieved by a chaotic system, which selects distinct invariant measures according to the class of external stimuli, is quite interesting and deserves further exploration. Inspired by the biological evidence a model has been developed [39], which behaves roughly as an olfactory system (in Freeman's sense) and, at the same time, is easier to describe and control by analytical means. To play the role of the local chaotic assembly of neurons a Bernoulli unit is chosen. The connection between the units is realized by linear synapses with an input correlation learning law and the external inputs also have adjustable gains, changing as in a biological potentiation mechanism. This last feature turns out to be useful to enhance the novelty-filter qualities of the system.

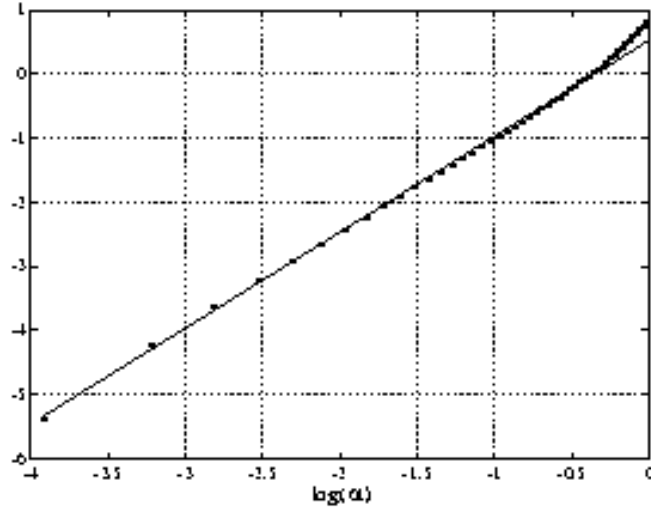


Figure 15:  $\log(-\log)$  of the characteristic function for the Weierstrass random walk ( $b=1.31$ )

### 3.1 A network of Bernoulli units

The network is the fully connected system shown in Fig.16. The output of the nodes is denoted by  $y_i$  and the  $x_i$ 's are the external inputs.  $W_{ij}$  with  $i, j \in \{1, 2, \dots, N\}$  are the connection strengths and  $W_{i0}$  are the input gains. Both  $W_{ij}$  and  $W_{i0}$  are real numbers in the interval  $[0, 1]$ . The input patterns are zero-one sequences  $(x_i \in \{0, 1\})$ . The learning laws for the connection strengths and the input gains are the following:

Let  $S_{ij}(t) = W_{ij}(t) + x_i(t)x_j(t)$ . Then for  $i \neq j$

$$W_{ij}(t+1) = S_{ij}(t) \text{ if } \sum_{k \neq i} S_{ik}(t) < C \quad (29)$$

$$W_{ij}(t+1) = C \frac{S_{ij}(t)}{\sum_{k \neq i} S_{ik}(t)} \text{ if } \sum_{k \neq i} S_{ik}(t) > C \quad (30)$$

for  $i = j$

$$W_{ii}(t+1) = 1 - \sum_{j \neq i} W_{ij}(t+1) \quad (31)$$

and for the input gains

$$W_{i0}(t+1) = \frac{N_i(1)_t}{N_i(1)_t + N_i(0)_t} \quad (32)$$

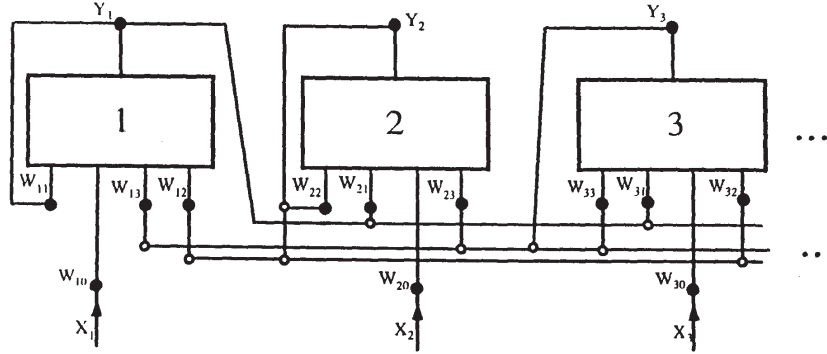


Figure 16: The Bernoulli network

According to Eqs.(29-32), when an input pattern has a one in both the  $i$  and  $j$  positions, the correlation of the units  $i$  and  $j$  becomes stronger.  $C < 1$  is a constant related to the node dynamics, which the sum of the off-diagonal connections is not allowed to exceed.  $C$  is a small parameter that controls the learning speed. Finally the diagonal element  $W_{ii}$  is chosen in such a way that the sum of all connections entering each unit adds to one.

In the input gain learning law,  $N_i(1)_t$  (or  $N_i(0)_t$ ) is the number of times that a one (or a zero) has appeared at the input  $i$ , up to time  $t$ . Eq.(32) means that if an input is excited many times, during the learning phase, it becomes more sensitive.

The node dynamics is

$$y_i(t+1) = f \left[ \sum_j W_{ij}(t)y_j(t) + W_{i0}x_i(t) \right] \quad (33)$$

$f$  being the function depicted in Fig.17.

The learning process starts with  $W_{ii} = 1$  and  $W_{ij} = 0$  for  $i \neq j$ . Each unit has then an independent absolutely continuous invariant measure which is the Lebesgue measure in  $[0;C]$  and zero outside. When the  $W_{ij}$  ( $i \neq j$ ) become different from zero but the inputs  $x_i$  are still zero, all variables  $y_i$  stay in the interval  $[0;C]$  because of the convex linear combination of inputs imposed by the normalization of the  $W_{ij}$ 's. When some inputs  $x_i$  are  $\neq 0$ , there is a finite probability for an irregular burst in the interval  $[C;1]$ , of some of the node variables, with reinjection into  $[0;C]$  whenever the iterate falls on the interval  $[\frac{1}{2} + \frac{C}{2}; \frac{1}{2} + C]$ .

The bursts in the interval  $[C;1]$ , in response to some of the input patterns, is the recognition mechanism of the network. The basal chaotic dynamics insuring a uniform covering of the interval  $[0;C]$ , the timing of the onset of the bursts depends only on the correlation probability and on the clock time of the discrete

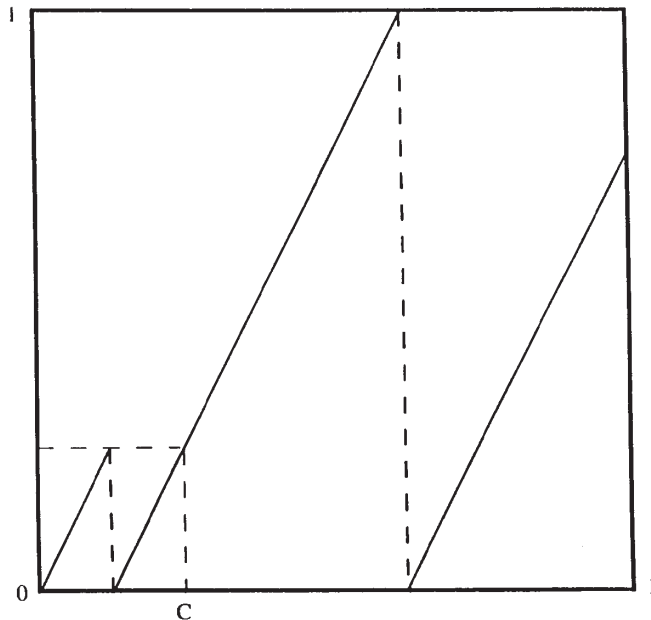


Figure 17: The node dynamics function

dynamics. We understand therefore why a chaos-based network may have a recognition time faster than an attractor network.

Learning, invariant measures and simulations

Both the connection strengths and the nature of the bursts, for a given set of  $W$ 's and an applied input pattern, may be estimated in probability.

In Eqs.(29-30), either the node  $i$  is not correlated to any other node and then all off-diagonal elements  $W_{ij}$  are zero or, as soon as the input patterns begin to correlate the node  $i$  with any other node, the off-diagonal elements start to grow and only the second case (Eq.(30)) needs to be considered. Let the learning gain be small. Then, in first order in  $\epsilon$ , we have

$$W_{ij}(t+1) = W_{ij}(t) + \epsilon \sum_{k \neq i} \frac{1}{C} W_{ij}(t) x_i(t)x_j(t) x_k(t)$$

For  $N$  learning steps, in first order in  $\epsilon$

$$W_{ij}(t+N) = W_{ij}(t) + \epsilon \sum_{n=0}^{N-1} x_i(t+n)x_j(t+n) \sum_{k \neq i} \frac{1}{C} W_{ij}(t) x_k(t+n)$$

Denoting by  $p_{ij}(1)$  the probability for the occurrence, in the input patterns, of a one both in the  $i$  and the  $j$  positions, the above equation has the stationary

solution

$$W_{ij} = C \frac{P_{ij}(1)}{\sum_{k \in i} P_{ik}(1)}$$

Now we establish an equation for the burst probabilities. Consider the case where  $C$  is much smaller than one, that is, the basal chaos is of low intensity. In this case, because of the normalization chosen for  $W_{ij}$ , the dynamics inside the interval  $[0; C]$  is dominated by  $y \rightarrow 2y \pmod{C}$  and in the interval  $[C; 1]$  by  $y \rightarrow 2y \pmod{1}$ . Hence, to a good approximation, we may assume uniform probability measures for the motion inside each one of the intervals. Denoting the interval  $[0; C]$  as the state 1 and the interval  $[C; 1]$  as the state 2, the dynamics of each node is a two-state Markov process with transition probabilities between the states corresponding to the probabilities of falling in some subintervals of the intervals  $[0; C]$  and  $[C; 1]$ . Namely, the probability  $p(2 \rightarrow 1)$  equals the probability of falling in the reinjection interval  $[\frac{1}{2} + \frac{C}{2}; \frac{1}{2} + C]$  and the probability  $p(1 \rightarrow 2)$  that of falling near the point  $C$  at a distance smaller than the off-diagonal excitation.

$$p_i(2 \rightarrow 1)_t = \frac{C}{2(1-C)} \quad (34)$$

$$p_i(2 \rightarrow 2)_t = 1 - p_i(2 \rightarrow 1)_t \quad (35)$$

$$p_i(1 \rightarrow 2)_t = \frac{1}{W_{ii}C} \left[ W_{i0}x_i(t) - C(1 - W_{ii}) + \sum_{j \in i} W_{ij}Y_j(t) \right] \quad (36)$$

$$p_i(1 \rightarrow 1)_t = 1 - p_i(1 \rightarrow 2)_t \quad (37)$$

where we have used the notation

$$f^\# = (f - 0)^+ - 1$$

for functions truncated to the range  $[0; 1]$ . That is,  $f^\# = 0$  if  $f < 0$ ,  $f^\# = 1$  if  $f > 1$  and  $f^\# = f$  if  $0 \leq f \leq 1$ .

The sum in the right-hand side of Eq.(36) is approximated in probability by

$$\sum_{j \in i} W_{ij} \left[ \frac{1}{2} p_j(2)_t + \frac{C}{2} (1 - p_j(2)_t) \right] \quad (38)$$

where  $p_j(2)_t$  denotes the probability of finding the node  $j$  in the state 2 at time  $t$ . The probability estimate (38), for the outputs  $y_j$ , assumes statistical independence of the units. This hypothesis fails when there are synchronization effects, which are to be expected mainly when a small group of units is strongly correlated.

With the probability estimate for the  $y_j$ 's and the detailed balance principle it is now possible to write a self-consistent equation for the probability  $p_i(2)_t$  to

and an arbitrary node  $i$  in the state 2 at time  $t$

$$p_i(2)_t = \frac{\frac{1}{W_{ii}C} W_{i0} x_i(t) + C(1 - W_{ii}) + \sum_{j \neq i} W_{ij} \frac{1}{2} p_j(2)_t + \frac{C}{2} (1 - p_j(2)_t)}{\frac{1}{W_{ii}C} W_{i0} x_i(t) + C(1 - W_{ii}) + \sum_{j \neq i} W_{ij} \frac{1}{2} p_j(2)_t + \frac{C}{2} (1 - p_j(2)_t)} + \frac{C}{2(1-C)} \quad (39)$$

For each input pattern  $x_i(t)$ , one obtains an estimate for  $p_i(2)_t$  solving Eq.(39) by iteration. We find that the solution that is obtained is qualitatively similar to the numerically determined invariant measures, although it tends to overestimate the burst excitation probabilities when they are small. This may be understood from the synchronization effects between groups of units. When one unit is not excited (not in state 2) the others tend also not to be excited, hence (38) overestimates the sum  $\sum_{j \neq i} W_{ij} y_j(t)$ .

We now illustrate how the network behaves as an associator and pattern recognizer. Consider, for display simplicity, a network of four nodes that is exposed during many iterations to the patterns 1000 and 0110 where the first pattern appears twice as much as the second. After this learning period we have exposed the network to all possible zero-one input patterns for 500 time steps each and observed the network reaction. During the recall experiment no further adjustment of the  $W_{ij}$ 's is made. The result is shown in the Fig.18.

The conclusions from this and other simulations is that, according to nature of the learning patterns, the network acts, for the recall input patterns, as a mixture of memory, associator and novelty filter. For example in Fig.18 we see that after having learned the sequences 1000 and 0110, the network reproduces these patterns as a memory. The pattern 1001 is associated to the pattern 1000 and the pattern 1110 associated to a mixture of the two learned patterns. By contrast the pattern 0100 is not recognized by the network which acts then as a novelty filter. Fig.19 shows the invariant measures of the system (expressed in probability per bin) when the input patterns are 1100 and 0110.

In conclusion, the network based on Bernoulli units, with node dynamics as in Fig.17 and correlation learning described by Eqs.(29-32):

1. Is a chaos-based pattern recognizer with the capability of operating on distinct invariant measures which are selected by the input patterns;
2. The response time of the selection is controlled by the magnitude of the invariant measures and the clock time of the basal chaotic dynamics;
3. As a pattern recognizer the network is a mixture of memory, associator and novelty filter. This however is sensitive to the learning algorithm that is chosen and, for the algorithm that is discussed here, it is sensitive also to value of the parameters  $C$  and  $\tau$ .

### 3.2 Feigenbaum networks

In this part one studies dynamical systems composed of a set of coupled quadratic maps

$$x_i(t+1) = 1 - \sum_j W_{ij} x_j(t) g^2 \quad (40)$$

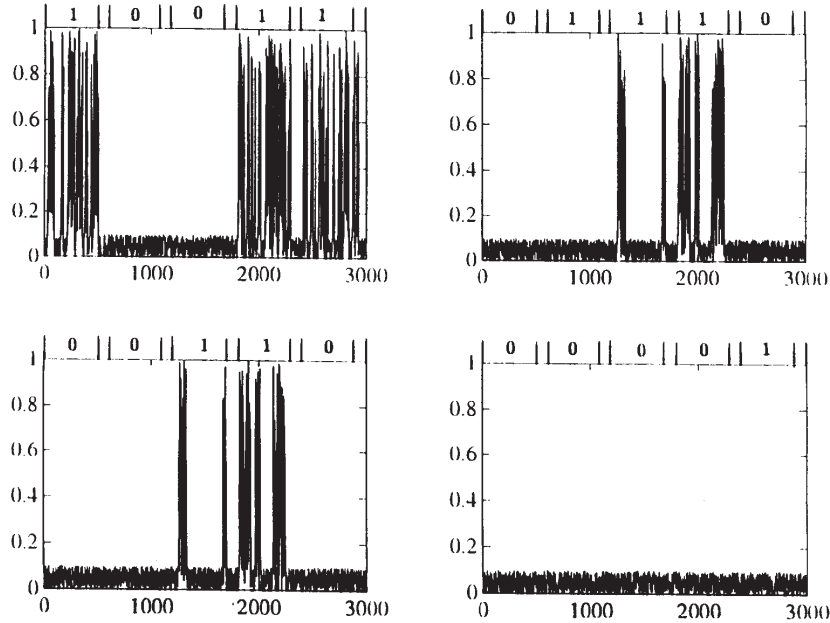


Figure 18: Response of a 4-nodes network after being exposed to the patterns 1000 and 0110 ( $C = 0.1$ ;  $\epsilon = 0.001$ )

with  $\times 2 \in [1;1]$ ,  $\sum_j W_{ij} = 1.8$  and  $W_{ij} > 0.8$  if  $i=j$  and  $= 1.401155\dots$ . The value chosen for  $\epsilon$  implies that, in the uncoupled limit ( $W_{ii} = 1; W_{ij} = 0 \text{ if } i \neq j$ ), each unit transforms as a one-dimensional quadratic map in the accumulation point of the Feigenbaum period-doubling bifurcation cascade. This system will be called a Feigenbaum network.

The quadratic map at the Feigenbaum accumulation point is not in the class of chaotic systems (in the sense of having positive Lyapunov exponents) however, it shares with them the property of having an infinite number of unstable periodic orbits. Therefore, before the interaction sets in, each elementary map possesses an infinite diversity of potential dynamical behaviors. As we will show later, the interaction between the individual units is able to selectively stabilize some of the previously unstable periodic orbits. The selection of the periodic orbits that are stabilized depends both on the initial conditions and on the intensity of the interaction coefficients  $W_{ij}$ . As a result Feigenbaum networks appear as systems with potential applications in the fields of control of chaos, information processing and as models of self-organization.

Control of chaos or of the transition to chaos has been, in recent years, a

very active field (see for example Ref. [40] and references therein). Several methods were developed to control the unstable periodic orbits that are embedded within a chaotic attractor. Having a way to select and stabilize at will these orbits we would have a device with infinite storage capacity (or infinite pattern discrimination capacity). However, an even better control might be achieved if, instead of an infinite number of unstable periodic orbits, the system possesses an infinite number of periodic attractors. The basins of attraction would evidently be small but the situation is in principle more favorable because the control need not be as sharp as before. As long as the system is kept in a neighborhood of an attractor the uncontrolled dynamics itself stabilizes the orbit.

The creation of systems with infinitely many sinks near an homoclinic tangency was discovered by Newhouse [41] and later studied by several other authors [42] [43] [44] [45] [46]. In the Newhouse phenomenon infinitely many attractors may coexist but only for special parameter values, namely for a residual subset of an interval. Another system, different from the Newhouse phenomena, which also displays many coexisting periodic attractors is a rotor map with a small amount of dissipation [47].

Here one shows that for a Feigenbaum system with only two units and symmetrical couplings one obtains a system which has an infinite number of sinks for an open set of coupling parameters. Then one also analyzes the behavior of a Feigenbaum network in the limit of a very large number of units. A mean field analysis shows the interaction between the units may generate distinct periodic orbit patterns throughout the network.

### 3.2.1 A simple system with an infinite number of sinks

Consider two units with symmetrical positive couplings ( $W_{12} = W_{21} = c > 0$ )

$$\begin{aligned} x_1(t+1) &= 1 - ((1-c)x_1(t) + cx_2(t))^2 \\ x_2(t+1) &= 1 - (cx_1(t) + (1-c)x_2(t))^2 \end{aligned} \quad (41)$$

The mechanism leading to the emergence of periodic attractors from a system that, without coupling, has no stable finite-period orbits is the permanence of the unstabilized orbits in a flip bifurcation and the contraction effect introduced by the coupling. The structure of the basins of attraction is also understood from the same mechanism. The result is [48]:

For sufficiently small  $c$  there is an  $N$  such that the system (41) has stable periodic orbits of all periods  $2^n$  for  $n > N$ .

### 3.2.2 Feigenbaum networks with many units

Mean-field analysis

For the calculations below it is convenient to use as variable the net input to the units,  $y_i = \sum_j W_{ij} x_j$ . Then Eq.(40) becomes,

$$y_i(t+1) = 1 - \sum_{j=1}^N W_{ij} y_j^2(t) \quad (42)$$

For practical purposes some restrictions have to be put on the range of values that the connection strengths may take. For information processing (pattern storage and pattern recognition) it is important to preserve, as much as possible, the dynamical diversity of the system. That means, for example, that a state with all the units synchronized is undesirable insofar as the effective number of degrees of freedom is drastically reduced. From

$$y_i(t+1) = \lambda y_i(t) (W_{ii} y_i(t) + \sum_{j \neq i} W_{ij} y_j(t)) \quad (43)$$

one sees that instability of the fully synchronized state implies  $\sum_{j \neq i} W_{ij} > 1$ . Therefore, the interesting case is when the off-diagonal connections are sufficiently small to insure that

$$W_{ii} > \frac{1}{\lambda} \quad (44)$$

For large  $N$ , provided there is no large scale synchronization effect, a mean-field analysis might be appropriate, at least to obtain qualitative estimates on the behavior of the network. For the unit  $i$  the average value  $\langle \sum_{j \neq i} W_{ij} y_j^2(t) \rangle$  acts like a constant and the mean-field dynamics is

$$z_i(t+1) = \lambda z_i(t) \quad (45)$$

where

$$z_i = \frac{y_i}{\langle \sum_{j \neq i} W_{ij} y_j^2 \rangle} \quad (46)$$

and

$$\lambda_{i,eff} = W_{ii} < \sum_{j \neq i} W_{ij} y_j^2 \rangle \quad (47)$$

$\lambda_{i,eff}$  is the effective parameter for the mean-field dynamics of unit  $i$ . From (44) and (47) it follows  $W_{ii} > \lambda_{i,eff} > W_{ii} \langle \sum_{j \neq i} W_{ij} y_j^2 \rangle$ . The conclusion is that the effective mean-field dynamics always corresponds to a parameter value below the Feigenbaum accumulation point, therefore, one expects the interaction to stabilize the dynamics of each unit in one of the  $2^n$ -periodic orbits. On the other hand to keep the dynamics inside an interesting region we require  $\lambda_{i,eff} > \lambda_2 = 1.3681$ , the period-2 bifurcation point. With the estimate  $\langle \sum_{j \neq i} W_{ij} y_j^2 \rangle = \frac{1}{3}$  one obtains

$$W_{ii} (1 - \frac{1}{3} (1 - W_{ii})) > \lambda_2 \quad (48)$$

which, together with (44), defines the interesting range of parameters for  $W_{ii} = \frac{1}{1 - \sum_{j \neq i} W_{ij}}$ .

Feigenbaum networks as signal processors

Let, for example, the  $W_{ij}$  connections be constructed from an input signal  $x_i$  by a correlation learning process

$$\begin{aligned} W_{ij} & \leftarrow W_{ij}^0 + x_i x_j e^{-\lambda} \quad \text{for } i \neq j \\ W_{ii} & \leftarrow W_{ii}^0 + \sum_{j \neq i} W_{ij} \end{aligned} \quad (49)$$

The dynamical behavior of the network, at a particular time, will reflect the learning history, that is, the data regularities, in the sense that  $W_{ij}$  is being structured by the patterns that occur more frequently in the data. The decay term  $e^{-\lambda}$  insures that the off-diagonal terms remain small and that the network structure is determined by the most frequent recent patterns. Alternatively, instead of the decay term, we might use a normalization method and the connection structure would depend on the weighted effect of all the data.

In the operating mode described above the network acts as a signal identifier. For example if the signal patterns are random, there is little correlation established and all the units operate near the Feigenbaum point. Alternatively the learning process may be stopped at a certain time and the network then used as a pattern recognizer. In this latter mode, whenever the pattern  $x_i x_j$  appears, one makes the replacement

$$\begin{aligned} W_{ij} & \leftarrow W_{ij}^0 + W_{ij} x_i x_j \quad \text{for } i \neq j \\ W_{ii} & \leftarrow W_{ii}^0 + \sum_{j \neq i} W_{ij} \end{aligned} \quad (50)$$

Therefore if  $W_{ij}$  was  $\neq 0$  but either  $x_i$  or  $x_j$  is 0 then  $W_{ij}^0 = 0$ . That is, the correlation between node  $i$  and  $j$  disappears and the effect of this connection on the lowering of the periods vanishes.

If both  $x_i$  and  $x_j$  are one, then  $W_{ij}^0 = W_{ij}$  and the effect of this connection persists. Suppose however that for all the  $W_{ij}$ 's different from zero either  $x_i$  or  $x_j$  are equal to zero. Then the correlations are totally destroyed and the network comes back to the uncorrelated (nonperiodic behavior). This case is what is called a novelty filter. Conversely, by displaying periodic behavior, the network recognizes the patterns that are similar to those that, in the learning stage, determined its connection structure. Recognition and association of similar patterns is then performed [48].

## References

- [1] M. Sato, Y. Murakami and K. Joe; Proc. Int. Conf. on Fuzzy Logic and Neural Networks, 601 (1990).
- [2] M. Sato, K. Joe and T. Hirahara; Proc. Int. Joint Conf. on Neural Networks, San Diego, vol. 1, p. 581 (1990)
- [3] B. A. Pearlmutter; Neural Computation, 1 (1989) 263.
- [4] T. Lin and B. G. Home; IEEE Trans. on Neural Networks, 7 (1996) 1329.

- [5] R. D. Jones; *Los Alamos Science*, 21 (1993) 195.
- [6] A. Amorim, R. Vilela Mendes and J. Seixas; *Learning Energy Correction Factors by Neural Networks: A Case Study for the ATLAS Calorimeter*, CERN report (1998).
- [7] F. J. Pineda; *Phys. Rev. Lett.* 59 (1987) 2229; *Neural Computation* 1 (1989) 161.
- [8] L. B. Almeida; *IEEE First Int. Conf. on Neural Networks*, M. Caudill and C. Butler (Eds.) p. 600 (1987).
- [9] L. B. Almeida; in *Neural Computers*, R. Eckmiller and Ch. von der Malsburg (Eds.) p. 199, Springer, Berlin 1988.
- [10] C. A. Skarda and W. J. Freeman; *Brain and Behavioral Science* 10 (1987) 161.
- [11] D. J. Amit and N. Brunel; *Network: Comput. in Neural Systems*, 8 (1997) 373.
- [12] A. V. M. Hertz; in *Models of Neural Networks III*, E. Domany, J. L. van Hemmen and K. Schulten (Eds.), p. 1, Springer.
- [13] S. Grossberg; *Neural Networks* 1 (1988) 17.
- [14] M. A. Cohen, S. Grossberg; *IEEE Transactions on Syst., Man and Cybern.*, 13 (1983) 815.
- [15] R. Vilela Mendes and J. T. Duarte; *Complex Systems* 6 (1992) 21.
- [16] R. Vilela Mendes and J. T. Duarte; *J. Math. Phys.*, 22 (1981) 1420.
- [17] J. J. Hopfield; *Proc. Nat. Acad. Sciences USA* 81 (1984) 3088.
- [18] F. C. Hoppensteadt and E. M. Izhikevich; *Weakly Connected Neural Networks*, Springer, Berlin 1997.
- [19] J. Doyne Farmer; *Physica D* 42 (1990) 153.
- [20] D. O. Hebb; *The organisation of behavior*, Wiley, New York, 1949.
- [21] T. D. Sanger; *Neural Networks* 2 (1989) 459.
- [22] E. Oja; *Int. J. of Neural Systems* 1 (1989) 61.
- [23] E. Oja; *Neural Networks* 5 (1992) 927.
- [24] J. A. Dente and R. Vilela Mendes; *Network: Computation in Neural Systems* 7 (1996) 123.
- [25] W. R. Softky and D. M. Kammen; *Neural Networks* 4 (1991) 337.

- [26] J. G. Taylor and S. Coombes; *Neural Networks* 6 (1993) 423.
- [27] E. Lukacs; *Characteristic functions*, Gri n, London 1970.
- [28] M. F. Shlesinger, G. M. Zaslavsky and J. K lafter, *Nature* 363 (1993) 31.
- [29] G. Zum ofen and J. K lafter, *Phys. Rev. E* 47 (1993) 851.
- [30] G. Zum ofen and J. K lafter, *Europhys. Lett.* 25 (1994) 565.
- [31] T. H ida, *Brownian motion*, Springer, Berlin 1980.
- [32] J. A. D ente and R. V ilela M endes; *Neural Networks* 10 (1997) 1465.
- [33] W. J. Freeman and B. Baird; *Behavioral Neuroscience* 101, 393 (1987)
- [34] W. J. Freeman; *Biological Cybernetics*, 56, 139 (1987)
- [35] W. J. Freeman, Y. Yao and B. Burke; *Neural Networks* 1, 277 (1988)
- [36] Y. Yao and W. J. Freeman; *Neural Networks* 3, 153 (1990)
- [37] Y. Yao, W. J. Freeman, B. Burke and Q. Yang; *Neural Networks* 4, 103 (1991)
- [38] D. J. Amit; "Modeling brain function. The world of attractor neural networks", Cambridge Univ. Press, Cambridge 1989
- [39] J. A. D ente and R. V ilela M endes; *Phys. Lett. A* 211 (1996) 87.
- [40] T. Shinbrot; *Advances in Physics* 44 (1995) 73.
- [41] S. E. Newhouse; *Topology* 13 (1974) 9; *Publ. Math. IHES* 50 (1979) 102.
- [42] C. Robinson; *Commun. Math. Phys.* 90 (1983) 433.
- [43] J. M. Gam baudo and C. Tresser; *J. Stat. Phys.* 32 (1983) 455.
- [44] L. Tedeschini-Lalli and J. A. Yorke; *Commun. Math. Phys.* 106 (1986) 635.
- [45] X.-J. Wang; *Commun. Math. Phys.* 131 (1990) 317.
- [46] H. E. Nusse and L. Tedeschini-Lalli; *Commun. Math. Phys.* 144 (1992) 429.
- [47] U. Feudel, C. Ge bogi, B. R. Hunt and J. A. Yorke; *Phys. Rev. E* 54 (1996) 71.
- [48] R. Carvalho, R. V ilela M endes and J. Seixas; *chao-dyn/9712004*, to appear in *Physica D* (1998).

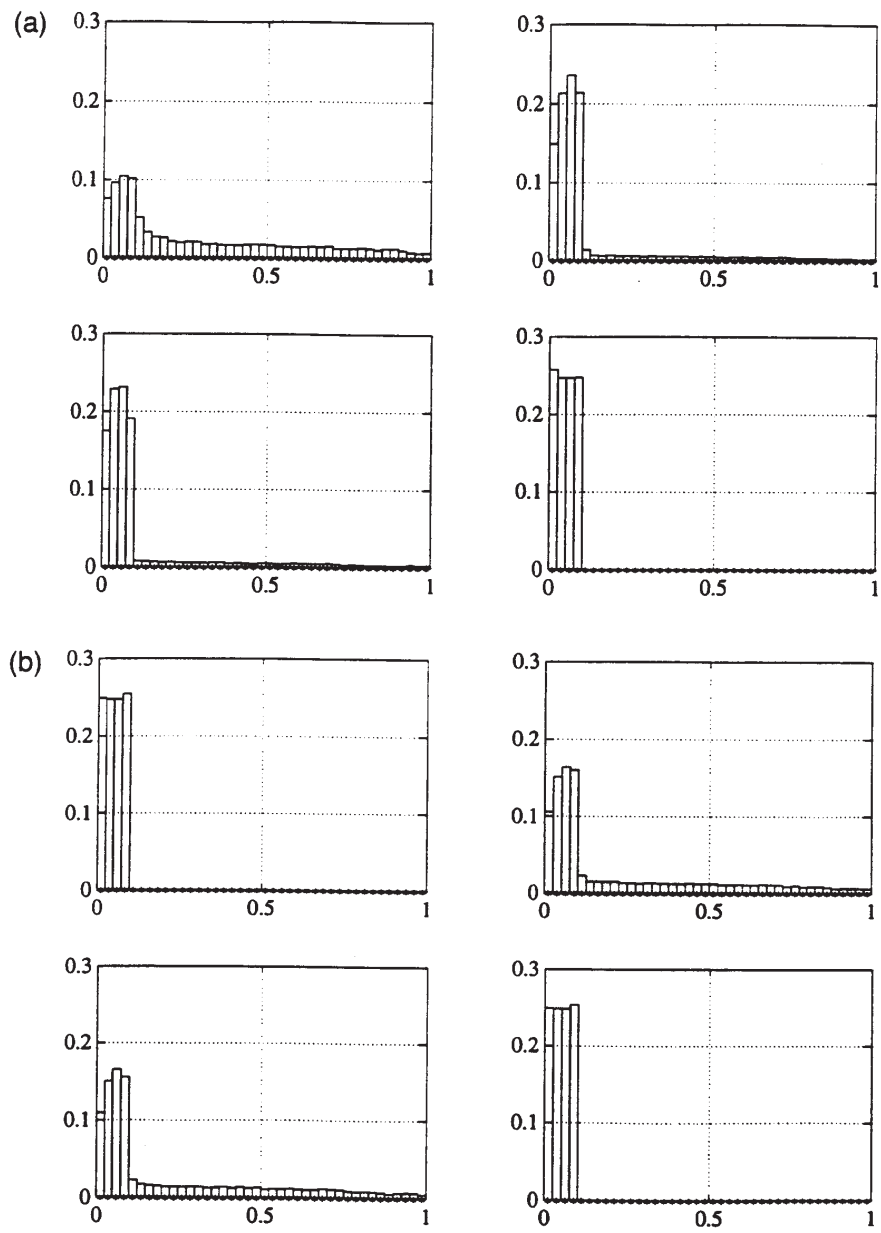


Figure 19: Invariant measures for the input patterns (a)1000 and (b)0110